

---

# Maximizing Cohesion and Separation in Graph Representation Learning: A Distance-aware Negative Sampling Approach

---

**M. Maruf**

Department of Computer Science,  
Virginia Tech  
Blacksburg, VA 24060  
marufm@vt.edu

**Anuj Karpatne**

Department of Computer Science,  
Virginia Tech  
Blacksburg, VA 24060  
karpatne@vt.edu

## Abstract

The objective of unsupervised graph representation learning (GRL) is to learn a low-dimensional space of node embeddings that reflect the structure of a given unlabeled graph. Existing algorithms for this task rely on negative sampling objectives that maximize the similarity in node embeddings at nearby nodes (referred to as “cohesion”) by maintaining positive and negative corpus of node pairs. While positive samples are drawn from node pairs that co-occur in short random walks, conventional approaches construct negative corpus by uniformly sampling random pairs, thus ignoring valuable information about structural dissimilarity among distant node pairs (referred to as “separation”). In this paper, we present a novel Distance-aware Negative Sampling (DNS) which maximizes the separation of distant node-pairs while maximizing cohesion at nearby node-pairs by setting the negative sampling probability proportional to the pair-wise shortest distances. Our approach can be used in conjunction with any GRL algorithm and we demonstrate the efficacy of our approach over baseline negative sampling methods over downstream node classification tasks on a number of benchmark datasets and GRL algorithms. All our codes and datasets are available at: <https://github.com/Distance-awareNS/DNS/>.

## 1 Introduction

The goal of graph representation learning (GRL) is to learn a low-dimensional vector embedding (or representation) of every node in the graph that captures the structure of interactions among nodes. The learned representations can be used as input features in several downstream tasks such as network classification, missing link prediction, or content recommendation. In GRL problems where every node has an associated set of attributes and target labels, e.g., over many benchmark datasets such as CiteSeer, Cora, and PubMed [Yang et al., 2016], one can employ supervised learning methods to extract node representations [Kipf and Welling, 2016a, Gilmer et al., 2017, García-Durán and Niepert, 2017, Hamilton et al., 2017, Veličković et al., 2017] that achieve state-of-the-art performance. However, in a general GRL problem, we may not always have access to node features or labels, or the node features may be available in complex and varying formats (e.g., as molecular structures in protein-protein interaction or drug-drug interaction graphs). Further, we may be interested in learning a “universal” embedding of the nodes that captures the graph structure and is independent of downstream supervised learning tasks. Such a universal representation can then be used as input features for a new downstream task without re-training the embeddings. For these reasons, we focus our attention to the problem of unsupervised GRL in this work, where the node representations are required to be learned solely from the graph structure (i.e., the adjacency matrix) and we do not

consider the presence of any node or edge attributes or labels. Henceforth, we will use the term GRL to refer to unsupervised GRL unless stated otherwise.

Most GRL algorithms are rooted in the idea of distributional similarity developed in the natural language processing (NLP) community [Mikolov et al., 2013], whereby words appearing in similar *contexts* (e.g., sentences in a document) are mapped to similar representations. In a similar vein, most of the existing GRL algorithms aim to maximize the similarity of embeddings at nearby nodes, which are assumed to belong to similar contexts based on the structure of the graph. This is generally performed by maintaining a *positive* corpus of nearby node-pairs (termed positive pairs) and a *negative* corpus of randomly sampled node-pairs (termed negative pairs). The similarity of embeddings over the positive corpus is then contrasted with that over the negative corpus, and their difference is maximized to ensure positive pairs occupy similar representations. A common strategy for sampling the negative pairs is by using a unigram distribution over all nodes, referred to as the unigram negative sampling (UNS) method.

While maximizing the similarity at nearby node-pairs is an important objective, a second objective that is important yet mostly overlooked in existing GRL algorithms is to maximize the *dissimilarity at distant node-pairs*. This is important because ideally, we would like to learn a graph embedding where the structural similarity of nodes in the graph (e.g., based on the distance of the shortest path between two nodes, or network distance) is preserved in the embedding space. In other words, the similarity of node-pairs in the embedding space should be proportional to the similarity of node-pairs in the graph (e.g., network distance). As a result, by maximizing this second objective, we can obtain well-separated and meaningful graph embeddings, whereby node-pairs that are nearby in the graph occupy similar representations while those that are far apart occupy dissimilar representations. Using an analogy from the domain of clustering, we refer to the first objective as maximizing *graph cohesion*, i.e., similarity at nearby nodes, and the second objective as maximizing *graph separation*, i.e., dissimilarity at distant nodes. We present an intuitive negative sampler for maximizing both cohesion and separation in GRL by sampling negative pairs with probability proportional to the distance between the nodes, termed as Distance-aware Negative Sampler (DNS).

**Our Contributions:** (1) We introduce and define the concepts of cohesion and separation in the context of GRL. (2) We propose a novel Distance-aware Negative Sampler (DNS) that maximizes both cohesion and separation. (3) We theoretically show the effectiveness of our DNS approach in maximizing cohesion and separation as compared to UNS. (4) We empirically show the ability of our DNS approach to learn meaningful representations, thus leading to better predictive performance on downstream ML tasks on several benchmark datasets in comparison with baseline GRL algorithms.

## 2 Related work

**Unsupervised graph representation learning methods:** A number of existing unsupervised GRL methods maximize embedding similarity at nearby nodes directly without performing negative sampling. Some examples include matrix factorization based methods [Ahmed et al., 2013, Cao et al., 2015, Ou et al., 2016] and skip-gram based methods [Perozzi et al., 2014, Abu-El-Haija et al., 2017, Armandpour et al., 2019]. Some GRL methods use a variety of negative sampling strategies to learn node embeddings. This category includes methods that use input node features such as Graph Convolutional Network (GCN) encoders [Kipf and Welling, 2016b, Hamilton et al., 2017, Veličković et al., 2018] that have achieved state-of-the-art performances on benchmark GRL datasets. However, they are not directly relevant to our GRL problem since we consider the formulation where no node features are available. Negative sampling based methods that do not use node features include node2vec [Grover and Leskovec, 2016], which optimizes random walk objectives and LINE [Tang et al., 2015], which uses first- or second-order neighborhoods to construct similar nodes. Note that while DeepWalk [Perozzi et al., 2014] was originally proposed using a Hierarchical Softmax objective, we can adapt it to construct a negative sampling based version of DeepWalk.

**Negative sampling strategies:** Here we discuss some of the common strategies for negative sampling that are at the basis of several unsupervised GRL algorithms. There are two generic types of negative samplers, edge-based [Kipf and Welling, 2016b, Tang et al., 2015] and node-based [Grover and Leskovec, 2016, Hamilton et al., 2017]. Edge-based samplers construct the positive corpus by selecting node pairs that have an edge between them, and the negative corpus by randomly selecting

node pairs that do not have an edge. On the other hand, node-based samplers use random walk objectives to construct the positive corpus and select random node pairs distributed with unigram distribution to construct the negative corpus. Among unigram distributions, two are common; one chooses negative samples with uniform probability [Kipf and Welling, 2016b, Tang et al., 2015] and the other uses degree-based probability [Grover and Leskovec, 2016, Hamilton et al., 2017], where the negative sampling probability is proportional to the  $\frac{3}{4}$ th power of the degree of each node. It is known that degree-based unigram sampler suffers from the *popular neighbor* problem [Armandpour et al., 2019], as this approach may choose a nearby node with high degree as a negative sample. Henceforth, by Unigram Negative Sampler (UNS), we refer the unigram sampler with uniform probability, and unigram-deg/UNS-deg denotes degree-based unigram negative sampler.

### 3 Preliminaries and problem objective

#### 3.1 Notations

We are given an undirected graph  $\mathcal{G} = (\mathcal{V}, \mathcal{E})$  where  $|\mathcal{V}| = n$ ,  $|\mathcal{E}| = m$ , and the adjacency matrix is given by  $\mathbf{A} = [a(i, j)]_{n \times n}$ . We assume that the graph is unweighted such that  $a(i, j) = 1$  iff  $(i, j) \in \mathcal{E}$ , otherwise 0. We denote the set of all possible node-pairs as  $\mathcal{S} = \mathcal{V} \times \mathcal{V}$ . Further, for every node-pair  $(i, j) \in \mathcal{S}$ , let us denote the distance or length of the shortest path between the nodes as  $d(i, j)$ . Incidentally,  $d(i, j) = 1$  iff  $(i, j) \in \mathcal{E}$ , i.e., there exists an edge between nodes  $i$  and  $j$ . Let us refer to the maximum value of  $d(i, j)$  in graph  $\mathcal{G}$  as  $d_{max}$ . We can then talk about the subset of node-pairs whose distance is equal to  $d$ , i.e.,  $\mathcal{S}_d = \{(i, j) \in \mathcal{S} | d(i, j) = d\}$ . It is easy to verify that  $\mathcal{S} = \mathcal{S}_0 \cup \mathcal{S}_1 \cup \dots \cup \mathcal{S}_{d_{max}}$  and  $\mathcal{S}_1 = \mathcal{E}$ .

With this setup, we consider the problem of unsupervised Graph Representation Learning (GRL) where the goal is to map every node  $i$  to an  $l$ -dimensional vector embedding,  $\mathbf{z}_i \in \mathbb{R}^l$ , such that the embedding space  $\mathcal{Z} = \{\mathbf{z}_i\}_{i=1}^n$  preserves the structural properties of nodes in graph  $\mathcal{G}$  (typically,  $l \ll |\mathcal{V}|$ ). In particular, we consider two generic types of measures in the embedding space of a pair of nodes, (i)  $\text{SIM}_{\mathcal{Z}}(i, j) :=$  similarity score between embeddings  $\mathbf{z}_i$  and  $\mathbf{z}_j$  (some examples include the dot product  $\mathbf{z}_i^T \mathbf{z}_j$  and its monotonic transformations  $\sigma(\mathbf{z}_i^T \mathbf{z}_j)$  and  $\log(\sigma(\mathbf{z}_i^T \mathbf{z}_j))$ , where  $\sigma$  denotes the sigmoid function), and (ii)  $\text{DISSIM}_{\mathcal{Z}}(i, j) :=$  dissimilarity score between embeddings  $\mathbf{z}_i$  and  $\mathbf{z}_j$  (some examples include  $-\mathbf{z}_i^T \mathbf{z}_j$ ,  $\sigma(-\mathbf{z}_i^T \mathbf{z}_j)$  and  $\log(\sigma(-\mathbf{z}_i^T \mathbf{z}_j))$ ). Note that there are multiple choices of similarity and dissimilarity functions to instantiate these two generic measures in any problem. Also, maximizing the similarity score of a node-pair is usually equivalent to minimizing its dissimilarity score for common function choices.

Ideally, we want to learn an embedding space  $\mathcal{Z}$  such that  $\text{SIM}_{\mathcal{Z}}(i, j)$  is large for nearby node-pairs in the graph (i.e., when  $d(i, j)$  is small) and  $\text{DISSIM}_{\mathcal{Z}}(i, j)$  is large for distant node-pairs (i.e., when  $d(i, j)$  is large). This objective, which is at the basis of the distributional hypothesis in linguistics [Harris, 1954], can be expressed using the notions of *cohesion* and *separation* in GRL, formally defined in the following.

#### 3.2 Cohesion and Separation

**Definition 1. Cohesion:** The cohesion of an embedding space  $\mathcal{Z}$  represents the aggregate similarity score between embeddings at nearby node-pairs in the graph. Formally, we define cohesion using the following weighted sum over similarity scores:

$$\text{COHESION}(\alpha, \mathcal{Z}) = \sum_{d=1}^{d_{max}} \alpha_d \sum_{(i,j) \in \mathcal{S}_d} \text{SIM}(i, j), \quad \text{where } \alpha_d \geq \alpha_{d+1}, \quad \alpha_d \geq 0 \quad \forall d.$$

Observe that since the weights  $\alpha_d$  monotonically decrease with  $d$ , this weighted sum pays greater emphasis to the similarity at nearby node-pairs (i.e.,  $\mathcal{S}_d$  with small  $d$ ). This is a generic definition of cohesion that can be instantiated using different choices of the weights  $\alpha$ . For example, if we specify  $\alpha_1 = 1$  and  $\alpha_d = 0 \quad \forall d > 1$ , then cohesion will be equal to the aggregate similarity over all the edges in  $\mathcal{G}$ . As we will see later, a common approach for specifying  $\alpha_d$  in most GRL algorithms is performing random walks and computing the probability of sampling a node-pair at a distance  $d$  in the random walk.

**Definition 2. Separation:** The separation of an embedding space  $\mathcal{Z}$  captures the aggregate dissimilarity between embeddings at distant node-pairs. Similar to cohesion, we can formally define

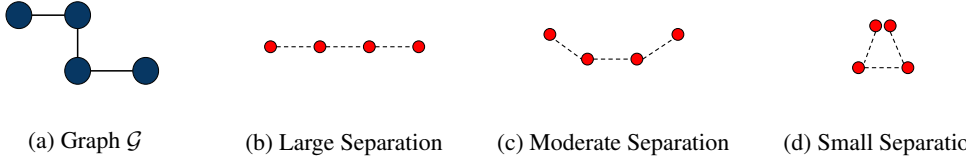


Figure 1: Mapping a toy graph (1a) into three different 2D-embedding spaces: (1b), (1c), and (1d). The position of each node denotes the 2D-embedding vector and the dotted lines represent edges in  $\mathcal{G}$ .

separation using the following weighted sum:

$$\text{SEPARATION}(\beta, \mathcal{Z}) = \sum_{d=1}^{d_{\max}} \beta_d \sum_{(i,j) \in \mathcal{S}_d} \text{DISSIM}(i, j), \quad \text{where } \beta_d \leq \beta_{d+1} \quad \beta_d \geq 0 \quad \forall d.$$

In this generic definition, since  $\beta_d$  monotonically increases with  $d$ , the dissimilarity at distant node-pairs have a greater contribution in the separation. Again, there can be multiple ways to instantiate  $\beta_d$ . For example, we can set  $\beta_{d_{\max}} = 1$  and  $\beta_d = 0 \forall d < d_{\max}$  such that the separation is equal to the dissimilarity at the farthest node-pairs in  $\mathcal{G}$ .

Since dissimilarity score is inversely related to similarity, it may seem that maximizing cohesion automatically maximizes separation. However, this is not true since the weighted sums involved in cohesion and separation focus on different subsets of node-pairs in  $\mathcal{S}$ : while cohesion focuses on  $\mathcal{S}_d$  for small  $d$ , separation focuses on node-pairs in  $\mathcal{S}_d$  for large  $d$ . We present the following theorem to prove this point.

**Theorem 1.** *Given two embedding spaces,  $\mathcal{Z}^1$  and  $\mathcal{Z}^2$ ,  $\text{COHESION}(\alpha, \mathcal{Z}^1) = \text{COHESION}(\alpha, \mathcal{Z}^2)$  does not imply that  $\text{SEPARATION}(\beta, \mathcal{Z}^1) = \text{SEPARATION}(\beta, \mathcal{Z}^2)$ , for all choices of  $\alpha$  and  $\beta$ .*

*Proof.* We use a counter-example to show that there can exist multiple embedding spaces such that their cohesion values are equal but their separation values are different. Figure 1a shows a toy graph with 4 nodes that is represented in three different two-dimensional embedding spaces in Figures 1b, 1c, and 1d. If we specify cohesion to be the aggregate similarity over edges (shown as dotted lines), we can see that all three embedding spaces have the same cohesion. However, if we define separation to be the aggregate dissimilarity at farthest nodes (at distance 3), we can see that the separation ranges from large (Figure 1b) to small (Figure 1d).  $\square$

### 3.3 GRL objective

As a result of Theorem 1, a GRL algorithm that only maximizes cohesion is not guaranteed to maximize separation and thus can lead to inferior embeddings such as the one shown in Figure 1d for the toy graph. This is one of the major drawbacks of skip-gram based GRL algorithms that only attempt to maximize the similarity at nearby nodes (where neighborhood is defined using random walks). We posit this as a natural consequence of the origin of these algorithms in natural language processing (NLP) applications, where the definition of distances between words (and hence the separation) is not as straight-forward as in graphs. We thus present a generalized objective of GRL using both cohesion and separation. We can show that existing GRL algorithms (e.g., unigram negative sampling based approaches) optimize special cases of this GRL objective.

**Definition 3. Generalized GRL Objective:** Given a graph  $\mathcal{G}$ , the goal of a GRL algorithm is to optimize the following generalized objective function with respect to  $\mathcal{Z}$ :

$$E(\mathcal{Z}) = \text{COHESION}(\alpha, \mathcal{Z}) + \text{SEPARATION}(\beta, \mathcal{Z}) \quad (1)$$

$$= \sum_{d=1}^{d_{\max}} \sum_{(i,j) \in \mathcal{S}_d} [\alpha_d \text{SIM}(i, j) + \beta_d \text{DISSIM}(i, j)] \quad (2)$$

$$\text{such that, } \frac{\alpha_1}{\beta_1} \gg 1, \quad \frac{\alpha_{d_{\max}}}{\beta_{d_{\max}}} \ll 1, \quad \text{and} \quad \frac{\beta_{d_{\max}}}{\beta_1} \gg 1 \quad (3)$$

Note that we do not use a trade-off parameter between cohesion and separation since any such parameter can be absorbed in  $\alpha$  or  $\beta$  as a constant multiplier. Different GRL algorithms optimize this generalized objective using different choices of similarity and dissimilarity functions, and settings of  $\alpha$  and  $\beta$  weights satisfying the GRL conditions in Equation 3. From the perspective of separation, we would prefer a GRL algorithm that employs a large value of  $\beta_{d_{max}}/\beta_1$ , such that the dissimilarity at farthest node-pairs is substantially larger than that of the nearest node-pairs. We call this fraction  $\beta_{d_{max}}/\beta_1$  as the **Separation Power** of a GRL algorithm.

## 4 Proposed method

**Negative sampling:** Before we present our proposed GRL algorithm based on the ideas of cohesion and separation, we formally discuss the generic family of negative sampling algorithms of which our algorithm is a special case. The objective function of negative sampling is given by the following equation:

$$\max_{\mathcal{Z}} \sum_{i \in \mathcal{V}} \sum_{j \in \mathcal{N}(i)} \underbrace{[\log \sigma(\mathbf{z}_i^T \mathbf{z}_j)]}_{\text{Positive Loss}} + K \sum_{k \in \mathcal{V}} \underbrace{P_{neg}(k|i) \log(\sigma(-\mathbf{z}_i^T \mathbf{z}_k))}_{\text{Negative Loss}}, \quad (4)$$

where node-pair  $(i, j)$  belongs to the positive corpus  $D_{pos}$  while  $(i, k)$  belongs to the negative corpus  $D_{neg}$ . We generally use random-walk strategy to construct  $D_{pos}$ , whereas  $D_{neg}$  is constructed by sampling  $K$  negative pairs  $(i, k)$  for each positive sample  $(i, j)$  with probability  $P_{neg}(k|i)$  [Mikolov et al., 2013, Gutmann and Hyvärinen, 2010]. A common choice of  $P_{neg}(k|i)$  is the unigram distribution that samples  $k$  with equal probability from all  $n$  nodes, referred as the Unigram Negative Sampling (UNS) algorithm.

The objective function of UNS can be shown to be a special case of the generalized GRL objective where the similarity at nearby nodes (i.e., cohesion) corresponds to the positive loss while the dissimilarity at distant nodes (i.e., separation) corresponds to the negative loss. However, a major limitation with UNS is that the probability of sampling a negative node-pair is independent of the distance between the nodes. As a result, UNS pays equal importance to the dissimilarity of node pairs with varying distances in the calculation of separation, thus leading to poor separation power. Theorem 2 provides a formal analysis of the correspondence of UNS to the generalized GRL objective and shows that its separation power is equal to 1.

**Theorem 2.** *Unigram Negative Sampling (UNS) Algorithm optimizes the generalized GRL objective with the following specifications:  $SIM(i, j) = \log(\sigma(\mathbf{z}_i^T \mathbf{z}_j))$ ,  $DISSIM(i, j) = \log(\sigma(-\mathbf{z}_i^T \mathbf{z}_j))$ ,  $\alpha_d = \pi_d(C, \mathbf{A})$ , where  $\pi_d(C, \mathbf{A})$  is the probability of sampling a node-pair at distance  $d$  using a  $C$ -length random walk on the graph with adjacency matrix  $\mathbf{A}$ , and  $\beta_d = KC/n$ . As a result, the Separation Power of UNS algorithm is equal to 1.*

*Proof.* Provided in the Supplementary material. □

**Distance-aware Negative Sampler:** We propose a Distance-aware Negative Sampler (DNS) which selects a negative sample  $k$  for node  $i$  using the sampling probability  $P_{neg}(k|i)$ , where  $P_{neg}(k|i)$  is linearly proportional to the pair-wise distance  $d(k, i)$ . Formally,

$$P_{neg}(k|i) \propto d(k, i)$$

$$P_{neg}(k|i) = \frac{d(k, i)}{\mathcal{D}(i, \mathbf{A})},$$

where  $\mathcal{D}(i, \mathbf{A})$  is the sum of distance of all node-pairs that contain node  $i$ ,  $\mathcal{D}(i, \mathbf{A}) = \sum_{s \in \mathcal{V}} d(s, i)$ . Let  $\mathcal{D}(\mathbf{A})$  be equal to  $\mathbb{E}_i(\mathcal{D}(i, \mathbf{A}))$ . Note that  $\mathcal{D}(\mathbf{A})$  depends on the average degree of the graph. For a fully connected graph,  $\mathcal{D}(\mathbf{A}) = n - 1$ . On the other extreme, when the graph is a chain of  $n$  nodes, then  $\mathcal{D}(\mathbf{A}) = \frac{n(n-1)}{2}$ . Generally, since most real world graphs are sparse,  $\mathcal{D}(\mathbf{A}) \gg n - 1$ . By construction, our proposed DNS approach has a separation power of  $d_{max}$  as stated in Theorem 3.

**Theorem 3.** *Distance-aware Negative Sampling (DNS) Algorithm optimizes the generalized GRL objective with the following specifications:  $SIM(i, j) = \log(\sigma(\mathbf{z}_i^T \mathbf{z}_j))$ ,  $DISSIM(i, j) =$*

$\log(\sigma(-\mathbf{z}_i^T \mathbf{z}_j))$ ,  $\alpha_d = \pi_d(C, \mathbf{A})$ , where  $\pi_d(C, \mathbf{A})$  is the probability of sampling a node-pair at distance  $d$  using a  $C$ -length random walk on the graph with adjacency matrix  $\mathbf{A}$ , and  $\beta_d = KCd/\mathcal{D}(\mathbf{A})$ . As a result, the Separation Power of DNS algorithm is equal to  $d_{max}$ .

*Proof.* Provided in the Supplementary material.  $\square$

**Corollary 1.** For UNS,  $(\frac{\alpha_d}{\beta_d})_{UNS} = \frac{\pi_d(C, \mathbf{A})n}{KC}$  and for DNS,  $(\frac{\alpha_d}{\beta_d})_{DNS} = \frac{\pi_d(C, \mathbf{A})\mathcal{D}(\mathbf{A})}{KCd}$ . Hence,  $(\frac{\alpha_d}{\beta_d})_{UNS} < (\frac{\alpha_d}{\beta_d})_{DNS}$  when  $n < \frac{\mathcal{D}(\mathbf{A})}{d}$ .

The above corollary helps us understand useful operating points of DNS. Since  $\mathcal{D}(\mathbf{A}) \gg n$  for most graphs, the  $(\alpha/\beta)$  ratio is generally always larger for DNS than UNS. We have also empirically observed that the  $(\alpha/\beta)$  ratio increases with  $C$  for all graphs considered in this work. As a result, DNS operates better at lower values of  $C$  since  $(\alpha/\beta)$  ratios remain small for moderate values of  $d$ . Also, DNS works better for sparse graphs where the nodes can be separated sufficiently.

The embedding space learned by DNS indeed preserves the graph-based similarity structure among nodes. Formally, Theorem 4 shows that the pairwise similarity in embedding space is a function of node-pair distance and for negative node-pairs, the similarity is inversely proportional to the distance.

**Theorem 4.** Let the average pairwise similarity for any two nodes at distance  $d$  be given by  $\xi_d = \frac{1}{|\mathcal{S}_d|} \text{SIM}(i, j) = \frac{1}{|\mathcal{S}_d|} \sum_{(i,j) \in \mathcal{S}_d} \sigma(z_i^T z_j)$ . We can then show that DNS generates embeddings such that  $\xi_d$  is a function of  $d$  and for  $d > C$ ,  $\xi_d$  is inversely proportional to  $d$ .

*Proof.* Provided in the Supplementary material.  $\square$

While negative sampling with linearly proportional distances is a simple heuristic, we can have a more general form of DNS by adding super-linearity or sub-linearity in the negative sampling probability which is,  $P_n(r|u) \propto (d(r, u))^\gamma$ . Here  $\gamma$  is a hyper-parameter and we can vary  $\gamma$  based on the properties of the dataset.

**Complexity analysis:** To compute the negative sampling probability, DNS requires pairwise distance information for all node pairs which is acquired using the shortest distance computation for all node pairs. For an arbitrary graph  $\mathcal{G} = (\mathcal{V}, \mathcal{E})$  where  $n = |\mathcal{V}|$  and  $m = |\mathcal{E}|$ , the time complexity to compute all pair shortest path length is  $\Theta(nm + n^2 \log n)$  [Dijkstra, 1959, Fredman and Tarjan, 1984] and the space complexity is  $\mathcal{O}(|n|^2)$  to store the normalized probability for all node pairs. Since we precompute the negative sampling probabilities for all node pairs before training the model, the training time complexity of DNS-based GRL is equal to the training time complexity of the UNS-based GRL yet DNS based model would require  $n^2$  more space to store the probabilities. Moreover, UNS-deg based model requires  $\mathcal{O}(n)$  space. We can consider an edge-based variant of DNS that does not need  $\mathcal{O}(n^2)$  space complexity at every training run. However, the current implementation performs node based sampling because the graphs are not too large.

## 5 Evaluation setup

**Benchmark datasets:** In our experiments, we use four benchmark datasets for node classification: CiteSeer, Cora, PubMed, and PPI [Yang et al., 2016, Zitnik and Leskovec, 2017] where CiteSeer, Cora, and PubMed are citation-networks and PPI is protein-protein interaction network. Since our goal is to find meaningful node-embeddings of a graph that only reflect the graph structure information rather than the node feature information, we do not use any node features of these benchmark datasets for our experiments. These datasets have multiple small disconnected components with the largest connected component that describes the graph structure properly. Consequently, our proposed DNS sampler requires a definite distance between any node pairs; therefore, we focus our experiments on the largest connected component of these networks. We provide a table in the Supplementary Materials that summarizes all the datasets with significant statistics where we see the citation networks are sparse and the PPI network is quite dense. Links to all codes and data used in this work are provided in the Supplementary Materials.

**Synthetic datasets.** We further analyze the representation quality of DNS-based GRL models with varying graph density using three synthetic datasets that have been generated using power-law

Table 1: The summary of the model performances in terms of downstream node classification F1-macro score. We highlight the best score for each dataset. For Cora, CiteSeer, PPI, and PubMed, we choose context window 4 to report the results. We run each model 5 times and report the performances in terms of mean and standard deviations. Whereas for some models, the standard deviations are negligible (close to zero).

Models	Dataset			
	CiteSeer	Cora	PubMed	PPI
GAE	$0.40 \pm 0.01$	$0.61 \pm 0.02$	$0.59 \pm 0.02$	0.68
VGAE	$0.39 \pm 0.02$	$0.58 \pm 0.02$	$0.60 \pm 0.02$	0.67
LINE	$0.37 \pm 0.05$	$0.52 \pm 0.05$	$0.47 \pm 0.07$	0.68
node2vec-UNS	$0.43 \pm 0.02$	$0.54 \pm 0.01$	$0.56 \pm 0.01$	0.63
<b>node2vec-DNS</b>	$0.52 \pm 0.01$	0.62	$0.58 \pm 0.01$	0.64
DeepWalk-UNS	$0.51 \pm 0.01$	0.67	0.58	<b>0.69</b>
DeepWalk-UNS-deg	0.47	$0.65 \pm 0.01$	0.54	0.68
<b>DeepWalk-DNS</b>	<b><math>0.61 \pm 0.01</math></b>	<b><math>0.72 \pm 0.01</math></b>	<b>0.63</b>	<b>0.69</b>

distribution and labeled using label propagation. A detailed analysis of network-generation and label-propagation for synthetic datasets are in the Supplementary Materials.

**Baseline models with hyperparameters:** For baseline models, we choose DeepWalk [Perozzi et al., 2014], node2vec [Grover and Leskovec, 2016], LINE [Tang et al., 2015], GAE [Kipf and Welling, 2016b] and VGAE [Kipf and Welling, 2016b] (details in Section 2). To evaluate the performance over each sampling approach, we implement the Unigram Negative Sampler and the Distance-aware Negative Sampler on DeepWalk and node2vec models. We set the embedding dimension as 128, the number of random walks per node as 50, and the number of negative samples as 20, whereas for node2vec model, we also set return parameter  $p$  as 1 and inout parameter  $q$  as 4 for our experiments. To optimize these models, we use Adam optimizer with 0.01 learning rate. Moreover, we run all node wise negative sampling-based GRL model for 30 epochs and all edgewise negative sampling base models for 400 epochs, as edgewise sampler models take more iterations to converge.

**Negative samplers:** For benchmark datasets, we evaluate the performance of our Distance-aware Negative Sampler with both types of Unigram Negative Samplers described in Section 2. We do an ablation study on our DNS sampler and a detailed discussion of its performance is in Supplementary Materials.

**Evaluation metrics:** To evaluate the embedding quality on the node-classification task, we use Logistic Regression (LR) with an lbfgs solver that supports 150 max iterations as our downstream model. For the PPI dataset, we use multi-class settings of LR. For benchmark datasets, we use the PyTorch Geometric [Fey and Lenssen, 2019] *train-test-validation* mask on the largest component to generate the training nodes, testing nodes and validation nodes. Meanwhile, for the synthetic datasets, we randomly select 10% nodes for training, 40% for validation, and 40% for testing. We use F1-Macro to report the classification accuracy as it gives equal importance to all classes, and hence preferred to use a metric for node classification. Moreover, we visualize the node representations using standard visualization tools like t-SNE, which is a dimensionality reduction technique that preserves local similarities.

## 5.1 Results

Table 1 compares the performance of our proposed DNS-based GRL models (DeepWalk-DNS and node2vec-DNS) with other baseline models on the benchmark node classification tasks. From the results, DNS-based models show a significant improvement in the F1-Macro score than that of the traditional sampling-based models across all benchmark datasets. Moreover, the t-SNE plot (Figure 2) shows that the DNS-based model learns more meaningful feature visualizations with better cohesion and separation of the classes (shown using colors) than that of the other models for CiteSeer dataset.

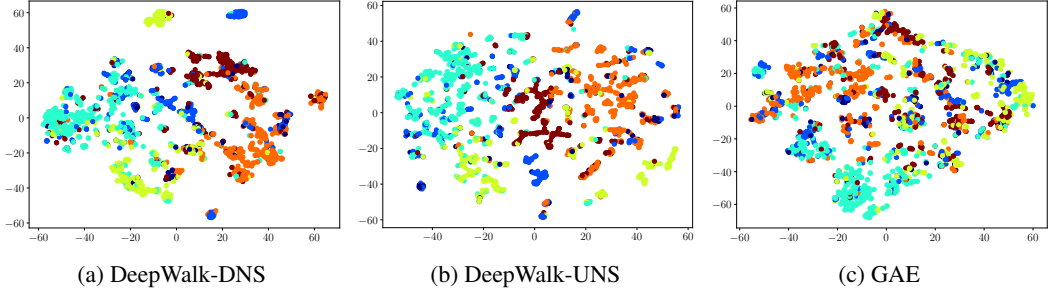


Figure 2: t-SNE plot for embeddings generated by DeepWalk with Distance-aware Negative Sampler model (DeepWalk-DNS), DeepWalk with Unigram Negative Sampler model (DeepWalk-UNS), and Graph Auto Encoder model (GAE) on CiteSeer dataset.

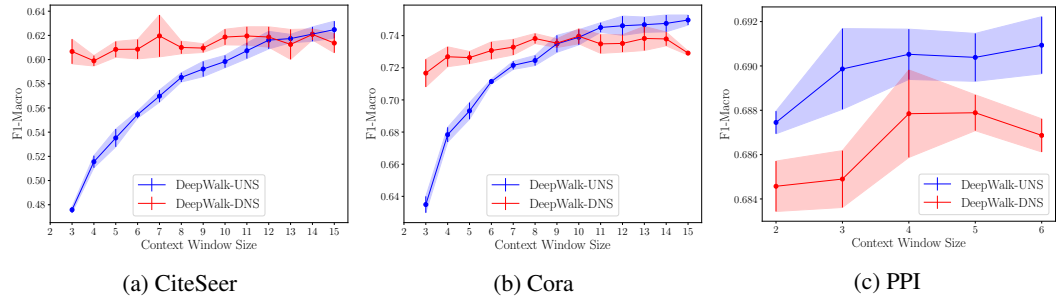


Figure 3: Node classification performance (measured by F1-Macro score) plot with varying context window on CiteSeer, Cora, and PPI dataset. DeepWalk with Distance-aware Negative Sampler (DeepWalk-DNS) and with Unigram Negative Sampler (DeepWalk-UNS) are the competing models.

To measure the impact of varying context windows on the DeepWalk-DNS and DeepWalk-UNS, we run experiments with varying context windows on Citeseer, Cora, and PPI datasets. Figure 3 shows node classification performance (F1-Macro score) of DeepWalk-DNS and DeepWalk-UNS with varying context windows, where the performance of DNS-based GRL model tends to get closer to UNS-based methods with increasing context window, which is in-line with our discussion in Section 4. However, we can see that the F1-score of DNS is significantly larger than that of UNS for a large range of context windows smaller than a reasonable value. In practice, we prefer low context windows during negative sampling for better optimization time at learning phase [Grover and Leskovec, 2016]. Moreover, for dense graphs, such as PPI, dissimilar nodes have low pairwise distances that weaken our node-similarity assumption and decrease DNS-based model performance. However, we can set the value of  $\gamma$  to a small value in  $\gamma$ -linear negative sampling, which reduces the effect of distances and improves performance for the densely connected graphs. We provide the details in Supplementary Materials.

Meanwhile, Figure 4 shows the similarity of the embeddings generated by DNS-based models on the synthetic graphs, which is inversely proportional to the pairwise distance that maximizes the separation of distant node pairs. A detailed analysis of DeepWalk-DNS on the synthetic dataset and the effect of  $\gamma$  in  $\gamma$ -linear negative sampling is in Supplementary Materials.

## 6 Conclusions and Future Work

This work presents a detailed discussion on Distance-aware Negative Sampling (DNS) for unsupervised Graph Representation Learning (GRL) where the node representations reflect graph structure better than the existing GRL methods by maximizing cohesion and separation on small and moderate graphs. With theoretical analysis on cohesion and separation and empirical results on the benchmark datasets, we present DNS sampler as state-of-the-art sampler that better optimizes the negative-sampling objective on unsupervised GRL. Future directions of this research could focus on the scalability of DNS to large graphs with disconnected components.

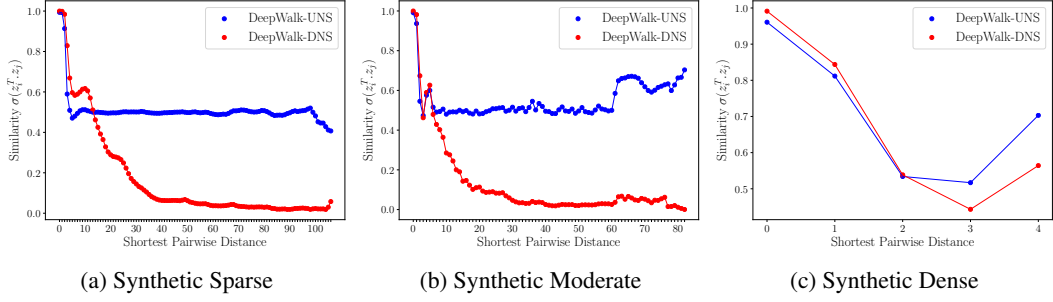


Figure 4: Average Pairwise Similarity of all node-pairs in embedding space where similarity =  $\sigma(z_i^T z_j)$  for  $z_i$  and  $z_j$  node embeddings. Embeddings generated by DNS based GRL model show minimum similarity for distant nodes with the similarity decreasing with increasing distance  $d$ .

## Broader Impact

This section provides a brief discussion of graph representation learning in real world applications and its impact on the society. Real world applications that incorporate interaction information to be represented in low-dimensional vector space use Graph Representation Learning. Among these applications, community detection and user role detection in social networks, user interest detection, content recommendation [Yang et al., 2011, Konstas et al., 2009, Backstrom and Leskovec, 2011, Liben-Nowell and Kleinberg, 2007] use graph representation learning to make prediction on interaction information. Moreover, graph representation learning has significant impacts to the scientific community by finding out complex chemical and molecular structure of compounds in chemical interaction graph [Gilmer et al., 2017], along with drug efficacy on different cells from drug-drug interaction graph [Stark et al., 2006, Zitnik and Leskovec, 2017, Radivojac et al., 2013]. Institutions with access of the interaction data can leverage these representation methods to make prediction for their interests. This paper redefines the objective function of unsupervised graph representation learning (GRL) in terms of Cohesion and Separation. Moreover, our proposed DNS sampler generates better graph representation by maximizing both cohesion and separation. DNS can be used in conjunction with any GRL method and can have better performance on downstream predictions. Based on the interaction graph, our proposed approach can have high impact on the prediction tasks of the above-mentioned networks.

## Supplementary Materials

In the first part of the Supplementary Materials, we provide the proofs of the stated theorems in Section 3 and Section 4. Later on, we provide details about the synthetic network generation and label propagation methodology and present additional results.

### Appendix A: Proofs of Theorems

**Theorem 2.** *Unigram Negative Sampling (UNS) Algorithm optimizes the generalized GRL objective with the following specifications:  $SIM(i, j) = \log(\sigma(\mathbf{z}_i^T \mathbf{z}_j))$ ,  $DISSIM(i, j) = \log(\sigma(-\mathbf{z}_i^T \mathbf{z}_j))$ ,  $\alpha_d = \pi_d(C, \mathbf{A})$ , where  $\pi_d(C, \mathbf{A})$  is the probability of sampling a node-pair at distance  $d$  using a  $C$ -length random walk on the graph with adjacency matrix  $\mathbf{A}$ , and  $\beta_d = KC/n$ . As a result, the Separation Power of UNS algorithm is equal to 1.*

*Proof.* To understand the relationship between the generalized GRL objective and UNS, let us look at the generic objective function of negative sampling (that applies for both UNS and DNS):

$$E(\mathcal{Z}) = \sum_{i \in \mathcal{V}} \sum_{j \in \mathcal{N}(i)} [\log \sigma(\mathbf{z}_i^T \mathbf{z}_j) + K \sum_{k \in \mathcal{V}} P_{neg}(k|i) \log(\sigma(-\mathbf{z}_i^T \mathbf{z}_k))] \quad (5)$$

where  $\mathcal{N}(i)$  represents the set of nodes (of size  $C$ ) that belong to the neighborhood of node  $i$  which we construct using random walk strategy. If we denote the probability of sampling a node  $j$  in a  $C$ -length random walk from  $i$  as  $P_{walk}(j|i)$ , then  $P_{walk}(j|i) = \pi_d(C, \mathbf{A})$ , where  $d$  is the distance between nodes  $i$  and  $j$ . The objective function of generic negative sampling can thus be written as:

$$E(\mathcal{Z}) = \sum_{i \in \mathcal{V}} \sum_{d=1}^{d_{max}} \sum_{j \in \mathcal{V} \wedge d(i,j)=d} \pi_d(C, \mathbf{A}) \log \sigma(\mathbf{z}_i^T \mathbf{z}_j) + \sum_{i \in \mathcal{V}} \sum_{j \in \mathcal{N}(i)} K \sum_{k \in \mathcal{V}} P_{neg}(k|i) \log(\sigma(-\mathbf{z}_i^T \mathbf{z}_k)) \quad (6)$$

$$= \sum_{d=1}^{d_{max}} \sum_{(i,j) \in \mathcal{S}_d} \pi_d(C, \mathbf{A}) \log \sigma(\mathbf{z}_i^T \mathbf{z}_j) + KC \sum_{i \in \mathcal{V}} \sum_{k \in \mathcal{V}} P_{neg}(k|i) \log(\sigma(-\mathbf{z}_i^T \mathbf{z}_k)) \quad (7)$$

$$= \sum_{d=1}^{d_{max}} \sum_{(i,j) \in \mathcal{S}_d} \pi_d(C, \mathbf{A}) \log \sigma(\mathbf{z}_i^T \mathbf{z}_j) + KC \sum_{d=1}^{d_{max}} \sum_{(i,j) \in \mathcal{S}_d} P_{neg}(k|i) \log(\sigma(-\mathbf{z}_i^T \mathbf{z}_k)) \quad (8)$$

In UNS,  $P_{neg}(j|i) = \frac{1}{n}$  where  $n$  is the number of nodes. Hence, the objective function for UNS becomes:

$$E(\mathcal{Z}) = \sum_{d=1}^{d_{max}} \sum_{(i,j) \in \mathcal{S}_d} \pi_d(C, \mathbf{A}) \log \sigma(\mathbf{z}_i^T \mathbf{z}_j) + \frac{KC}{n} \sum_{d=1}^{d_{max}} \sum_{(i,j) \in \mathcal{S}_d} \log(\sigma(-\mathbf{z}_i^T \mathbf{z}_j)) \quad (9)$$

$$= \sum_{d=1}^{d_{max}} \sum_{(i,j) \in \mathcal{S}_d} [\pi_d(C, \mathbf{A}) \log \sigma(\mathbf{z}_i^T \mathbf{z}_j) + \frac{KC}{n} \log(\sigma(-\mathbf{z}_i^T \mathbf{z}_j))] \quad (10)$$

$$= \sum_{d=1}^{d_{max}} \sum_{(i,j) \in \mathcal{S}_d} [\alpha_d \text{SIM}(i, j) + \beta_d \text{DISSIM}(i, j)] \quad (11)$$

where,  $\text{SIM}(i, j) = \log(\sigma(\mathbf{z}_i^T \mathbf{z}_j))$ ,  $\text{DISSIM}(i, j) = \log(\sigma(-\mathbf{z}_i^T \mathbf{z}_j))$ ,  $\alpha_d = \pi_d(C, \mathbf{A})$ , and  $\beta_d = KC/n$ . Clearly, Equation 11 corresponds to the generalized GRL objective. The Separation Power of UNS is equal to  $\frac{\beta_{d_{max}}}{\beta_1} = \frac{KC/n}{KC/n} = 1$ .  $\square$

**Theorem 3.** *Distance-aware Negative Sampling (DNS) Algorithm optimizes the generalized GRL objective with the following specifications:  $SIM(i, j) = \log(\sigma(\mathbf{z}_i^T \mathbf{z}_j))$ ,  $DISSIM(i, j) = \log(\sigma(-\mathbf{z}_i^T \mathbf{z}_j))$ ,  $\alpha_d = \pi_d(C, \mathbf{A})$ , where  $\pi_d(C, \mathbf{A})$  is the probability of sampling a node-pair at distance  $d$  using a  $C$ -length random walk on the graph with adjacency matrix  $\mathbf{A}$ , and  $\beta_d = KCd/\mathcal{D}(\mathbf{A})$ . As a result, the Separation Power of DNS algorithm is equal to  $d_{max}$ .*

*Proof.* For Distance-aware Negative Sampler (DNS), the negative sampling probability  $P_{neg}(j|i)$  is linearly proportional to the pair-wise distance  $d(j, i)$ ;  $P_{neg}(j|i) = \frac{d(j, i)}{\mathcal{D}(i, \mathbf{A})} = \frac{d}{\mathcal{D}(i, \mathbf{A})}$ . We approximate the expected value of  $\mathcal{D}(i, \mathbf{A})$  as  $\mathcal{D}(\mathbf{A})$ . The objective function for DNS can thus be obtained by substituting the value of  $P_{neg}(j|i)$  in Equation 8 as follows:

$$E(\mathcal{Z}) = \sum_{d=1}^{d_{max}} \sum_{(i,j) \in \mathcal{S}_d} \pi_d(C, \mathbf{A}) \log \sigma(\mathbf{z}_i^T \mathbf{z}_j) + \sum_{d=1}^{d_{max}} \sum_{(i,j) \in \mathcal{S}_d} KC \frac{d}{\mathcal{D}(\mathbf{A})} \log(\sigma(-\mathbf{z}_i^T \mathbf{z}_j)) \quad (12)$$

$$= \sum_{d=1}^{d_{max}} \sum_{(i,j) \in \mathcal{S}_d} [\pi_d(C, \mathbf{A}) \log \sigma(\mathbf{z}_i^T \mathbf{z}_j) + \frac{KCd}{\mathcal{D}(\mathbf{A})} \log(\sigma(-\mathbf{z}_i^T \mathbf{z}_j))] \quad (13)$$

$$= \sum_{d=1}^{d_{max}} \sum_{(i,j) \in \mathcal{S}_d} [\alpha_d \text{SIM}(i, j) + \beta_d \text{DISSIM}(i, j)] \quad (14)$$

where,  $\text{SIM}(i, j) = \log(\sigma(\mathbf{z}_i^T \mathbf{z}_j))$ ,  $\text{DISSIM}(i, j) = \log(\sigma(-\mathbf{z}_i^T \mathbf{z}_j))$ ,  $\alpha_d = \pi_d(C, \mathbf{A})$ , and  $\beta_d = KCd/\mathcal{D}(\mathbf{A})$ . Clearly, Equation 14 corresponds to the generalized GRL objective. The Separation Power of DNS is equal to  $\frac{\beta_{d_{max}}}{\beta_1} = \frac{KCd_{max}/\mathcal{D}(\mathbf{A})}{KC/\mathcal{D}(\mathbf{A})} = d_{max}$ .  $\square$

**Theorem 4.** Let the average pairwise similarity for any two nodes at distance  $d$  be given by  $\xi_d = \frac{1}{|\mathcal{S}_d|} \text{SIM}(i, j) = \frac{1}{|\mathcal{S}_d|} \sum_{(i,j) \in \mathcal{S}_d} \sigma(\mathbf{z}_i^T \mathbf{z}_j)$ . We can then show that DNS generates embeddings such that  $\xi_d$  is a function of  $d$  and for  $d > C$ ,  $\xi_d$  is inversely proportional to  $d$ .

*Proof.* Let us assume that the DNS based GRL model has reached its global maximum with loss  $\mathcal{Q}$ . From Equation 12, the loss of DNS based GRL model is given by,

$$\mathcal{Q} = - \sum_{d=1}^{d_{max}} \sum_{(i,j) \in \mathcal{S}_d} \pi_d(C, \mathbf{A}) \log \sigma(\mathbf{z}_i^T \mathbf{z}_j) - KC \sum_{d=1}^{d_{max}} \sum_{(i,j) \in \mathcal{S}_d} \frac{d}{\mathcal{D}(\mathbf{A})} \log(\sigma(-\mathbf{z}_i^T \mathbf{z}_j)) \quad (15)$$

$$= - \sum_{d=1}^{d_{max}} \sum_{(i,j) \in \mathcal{S}_d} \pi_d(C, \mathbf{A}) \log \sigma(\mathbf{z}_i^T \mathbf{z}_j) - KC \sum_{d=1}^{d_{max}} \sum_{(i,j) \in \mathcal{S}_d} \frac{d}{\mathcal{D}(\mathbf{A})} \log(1 - \sigma(\mathbf{z}_i^T \mathbf{z}_j)) \quad (16)$$

Since the model has reached its global optimum, the similarity  $\sigma(\mathbf{z}_i^T \mathbf{z}_j)$  for nearby node-pairs ( $d(i, j) < C$ ) should be high such that  $1 - \sigma(\mathbf{z}_i^T \mathbf{z}_j)$  low. We approximate  $\log(\sigma(\mathbf{z}_i^T \mathbf{z}_j)) \approx \sigma(\mathbf{z}_i^T \mathbf{z}_j) - 1$  as the remainder term in its Taylor's series expansion is close to zero. Moreover, we expand  $\log(1 - \sigma(\mathbf{z}_i^T \mathbf{z}_j)) = -\sigma(\mathbf{z}_i^T \mathbf{z}_j) - \frac{\sigma(\mathbf{z}_i^T \mathbf{z}_j)^2}{2} - \frac{\sigma(\mathbf{z}_i^T \mathbf{z}_j)^3}{3} - \dots = -\sigma(\mathbf{z}_i^T \mathbf{z}_j) - \mathcal{R}(\sigma(\mathbf{z}_i^T \mathbf{z}_j))$ . Note that the length of the random walk is at most  $C$ . Consequently, for  $d > C$ ,  $\pi_d(C, \mathbf{A}) = 0$ . We can thus rearrange Equation 16 as,

$$\begin{aligned} \mathcal{Q} &= - \sum_{d=1}^C \sum_{(i,j) \in \mathcal{S}_d} \pi_d(C, \mathbf{A}) (\sigma(\mathbf{z}_i^T \mathbf{z}_j) - 1) \\ &\quad - KC \sum_{d=1}^{d_{max}} \sum_{(i,j) \in \mathcal{S}_d} \frac{d}{\mathcal{D}(\mathbf{A})} (-\sigma(\mathbf{z}_i^T \mathbf{z}_j) - \mathcal{R}(\sigma(\mathbf{z}_i^T \mathbf{z}_j))) \\ &= - \sum_{d=1}^C \sum_{(i,j) \in \mathcal{S}_d} \pi_d(C, \mathbf{A}) (\sigma(\mathbf{z}_i^T \mathbf{z}_j) - 1) \\ &\quad + KC \sum_{d=1}^{d_{max}} \sum_{(i,j) \in \mathcal{S}_d} \left( \frac{d}{\mathcal{D}(\mathbf{A})} \sigma(\mathbf{z}_i^T \mathbf{z}_j) + \frac{d}{\mathcal{D}(\mathbf{A})} \mathcal{R}(\sigma(\mathbf{z}_i^T \mathbf{z}_j)) \right) \end{aligned}$$

We approximate  $\frac{d}{\mathcal{D}(\mathbf{A})} \mathcal{R}(\sigma(\mathbf{z}_i^T \mathbf{z}_j)) \approx 0$  because  $R(\sigma(\mathbf{z}_i^T \mathbf{z}_j)) \approx 0$  for distant pairs and  $\frac{d}{\mathcal{D}(\mathbf{A})} \approx 0$  for nearby pairs at optimum. Hence, we obtain:

$$\begin{aligned}
\mathcal{Q} &= - \sum_{d=1}^C \sum_{(i,j) \in \mathcal{S}_d} \pi_d(C, \mathbf{A}) \sigma(\mathbf{z}_i^T \mathbf{z}_j) + \sum_{d=1}^C \sum_{(i,j) \in \mathcal{S}_d} \pi_d(C, \mathbf{A}) \\
&\quad + KC \sum_{d=1}^{d_{max}} \sum_{(i,j) \in \mathcal{S}_d} \frac{d}{\mathcal{D}(\mathbf{A})} \sigma(\mathbf{z}_i^T \mathbf{z}_j) \\
&= \sum_{d=1}^C \sum_{(i,j) \in \mathcal{S}_d} \pi_d(C, \mathbf{A}) - \sum_{d=1}^C \sum_{(i,j) \in \mathcal{S}_d} \left( \pi_d(C, \mathbf{A}) - \frac{KCd}{\mathcal{D}(\mathbf{A})} \right) \sigma(\mathbf{z}_i^T \mathbf{z}_j) \\
&\quad + \sum_{d=C+1}^{d_{max}} \sum_{(i,j) \in \mathcal{S}_d} \frac{KCd}{\mathcal{D}(\mathbf{A})} \sigma(\mathbf{z}_i^T \mathbf{z}_j)
\end{aligned} \tag{17}$$

For  $d \leq C$ , we rearrange Equation 17 as,

$$\begin{aligned}
\mathcal{Q} &= \sum_{d'=1}^C \sum_{(i,j) \in \mathcal{S}_{d'}} \pi_{d'}(C, \mathbf{A}) - \sum_{d'=1}^C \sum_{(i,j) \in \mathcal{S}_{d'}} \left( \pi_{d'}(C, \mathbf{A}) - \frac{KCd'}{\mathcal{D}(\mathbf{A})} \right) \sigma(\mathbf{z}_i^T \mathbf{z}_j) \\
&\quad + \sum_{d'=C+1}^{d_{max}} \sum_{(i,j) \in \mathcal{S}_{d'}} \frac{KCd'}{\mathcal{D}(\mathbf{A})} \sigma(\mathbf{z}_i^T \mathbf{z}_j) \\
&= \sum_{d'=1}^C \sum_{(i,j) \in \mathcal{S}_{d'}} \pi_{d'}(C, \mathbf{A}) - \sum_{(i,j) \in \mathcal{S}_d} \left( \pi_d(C, \mathbf{A}) - \frac{KCd}{\mathcal{D}(\mathbf{A})} \right) \sigma(\mathbf{z}_i^T \mathbf{z}_j) \\
&\quad - \sum_{\substack{d'=1 \\ d' \neq d}}^{d_{max}} \sum_{(i,j) \in \mathcal{S}_{d'}} \left( \pi_{d'}(C, \mathbf{A}) - \frac{KCd'}{\mathcal{D}(\mathbf{A})} \right) \sigma(\mathbf{z}_i^T \mathbf{z}_j) + \sum_{d'=C+1}^{d_{max}} \sum_{(i,j) \in \mathcal{S}_{d'}} \frac{KCd'}{\mathcal{D}(\mathbf{A})} \sigma(\mathbf{z}_i^T \mathbf{z}_j) \\
&= \sum_{d'=1}^C \sum_{(i,j) \in \mathcal{S}_{d'}} \pi_{d'}(C, \mathbf{A}) - \left( \pi_d(C, \mathbf{A}) - \frac{KCd}{\mathcal{D}(\mathbf{A})} \right) |\mathcal{S}_d| \xi_d \\
&\quad - \sum_{\substack{d'=1 \\ d' \neq d}}^{d_{max}} \sum_{(i,j) \in \mathcal{S}_{d'}} \left( \pi_{d'}(C, \mathbf{A}) - \frac{KCd'}{\mathcal{D}(\mathbf{A})} \right) \sigma(\mathbf{z}_i^T \mathbf{z}_j) + \sum_{d'=C+1}^{d_{max}} \sum_{(i,j) \in \mathcal{S}_{d'}} \frac{KCd'}{\mathcal{D}(\mathbf{A})} \sigma(\mathbf{z}_i^T \mathbf{z}_j)
\end{aligned}$$

$$\begin{aligned}
\xi_d &= \frac{1}{|\mathcal{S}_d| \left( \pi_d(C, \mathbf{A}) - \frac{KCd}{\mathcal{D}(\mathbf{A})} \right)} \times \left[ -\mathcal{Q} + \sum_{d'=1}^C \sum_{(i,j) \in \mathcal{S}_{d'}} \pi_{d'}(C, \mathbf{A}) \right. \\
&\quad \left. - \sum_{\substack{d'=1 \\ d' \neq d}}^{d_{max}} \sum_{(i,j) \in \mathcal{S}_{d'}} \left( \pi_{d'}(C, \mathbf{A}) - \frac{KCd'}{\mathcal{D}(\mathbf{A})} \right) \sigma(\mathbf{z}_i^T \mathbf{z}_j) + \sum_{d'=C+1}^{d_{max}} \sum_{(i,j) \in \mathcal{S}_{d'}} \frac{KCd'}{\mathcal{D}(\mathbf{A})} \sigma(\mathbf{z}_i^T \mathbf{z}_j) \right]
\end{aligned}$$

From the above Equation,  $\xi_d = f(d, \Theta)$  for  $d \leq C$ , where  $\Theta$  is the set of parameters of  $f$  other than  $d$ .

Table 2: Summary statistics of the datasets we used for experiments where we choose the largest connected components from 390 components for CiteSeer and 78 components for Cora (PubMed and PPI are single connected component graph). We represent the largest component as  $\mathcal{G} = (\mathcal{V}, \mathcal{E})$  and the set of unique class labels as  $y$ . PPI dataset has 121 multi-classes with binary labels. The average node degree is represented by  $\overline{deg}$ , and the maximum node pair distance is denoted by  $d_{MAX}$ .

Stat	CiteSeer	Cora	PubMed	PPI	Syn. Sparse	Syn. Moderate	Syn. Dense
$ \mathcal{V} $	2,120	2,485	19,717	2,339	2,000	2,000	2,000
$ \mathcal{E} $	7,358	10,138	88,648	65,430	4,982	12,062	30,472
$ y $	6	7	3	121	7	5	4
$d_{MAX}$	28	19	18	7	106	82	4
$\overline{deg}$	3.47	4.08	4.5	27.97	2.49	6.03	15.24

For  $d > C$ , we rearrange Equation 17 as,

$$\begin{aligned}
\mathcal{Q} &= \sum_{d'=1}^C \sum_{(i,j) \in \mathcal{S}_{d'}} \pi_{d'}(C, \mathbf{A}) - \sum_{d'=1}^C \sum_{(i,j) \in \mathcal{S}_{d'}} \left( \pi_{d'}(C, \mathbf{A}) - \frac{KCd'}{\mathcal{D}(\mathbf{A})} \right) \sigma(\mathbf{z}_i^T \mathbf{z}_j) \\
&\quad + \sum_{d'=C+1}^{d_{max}} \sum_{(i,j) \in \mathcal{S}_{d'}} \frac{KCd'}{\mathcal{D}(\mathbf{A})} \sigma(\mathbf{z}_i^T \mathbf{z}_j) \\
&= \sum_{d'=1}^C \sum_{(i,j) \in \mathcal{S}_{d'}} \pi_{d'}(C, \mathbf{A}) - \sum_{d'=1}^C \sum_{(i,j) \in \mathcal{S}_{d'}} \left( \pi_{d'}(C, \mathbf{A}) - \frac{KCd'}{\mathcal{D}(\mathbf{A})} \right) \sigma(\mathbf{z}_i^T \mathbf{z}_j) \\
&\quad + \sum_{(i,j) \in \mathcal{S}_d} \frac{KCd}{\mathcal{D}(\mathbf{A})} \sigma(\mathbf{z}_i^T \mathbf{z}_j) + \sum_{d'=C+1}^{d_{max}} \sum_{\substack{(i,j) \in \mathcal{S}_{d'} \\ d' \neq d}} \frac{KCd'}{\mathcal{D}(\mathbf{A})} \sigma(\mathbf{z}_i^T \mathbf{z}_j) \\
&= \sum_{d'=1}^C \sum_{(i,j) \in \mathcal{S}_{d'}} \pi_{d'}(C, \mathbf{A}) - \sum_{d'=1}^C \sum_{(i,j) \in \mathcal{S}_{d'}} \left( \pi_{d'}(C, \mathbf{A}) - \frac{KCd'}{\mathcal{D}(\mathbf{A})} \right) \sigma(\mathbf{z}_i^T \mathbf{z}_j) \\
&\quad + \frac{KCd}{\mathcal{D}(\mathbf{A})} |\mathcal{S}_d| \xi_d + \sum_{d'=C+1}^{d_{max}} \sum_{\substack{(i,j) \in \mathcal{S}_{d'} \\ d' \neq d}} \frac{KCd'}{\mathcal{D}(\mathbf{A})} \sigma(\mathbf{z}_i^T \mathbf{z}_j) \\
\xi_d &= \frac{\mathcal{D}(\mathbf{A})}{|\mathcal{S}_d| KC d} [ \mathcal{Q} - \sum_{d'=1}^C \sum_{(i,j) \in \mathcal{S}_{d'}} \pi_{d'}(C, \mathbf{A}) \\
&\quad + \sum_{d'=1}^C \sum_{(i,j) \in \mathcal{S}_{d'}} \left( \pi_{d'}(C, \mathbf{A}) - \frac{KCd'}{\mathcal{D}(\mathbf{A})} \right) \sigma(\mathbf{z}_i^T \mathbf{z}_j) - \sum_{d'=C+1}^{d_{max}} \sum_{\substack{(i,j) \in \mathcal{S}_{d'} \\ d' \neq d}} \frac{KCd'}{\mathcal{D}(\mathbf{A})} \sigma(\mathbf{z}_i^T \mathbf{z}_j) ]
\end{aligned}$$

From the above Equation,  $\xi_d$  is inversely proportional to  $d$  for  $d > C$ .  $\square$

## Appendix B: Result Analysis

All our codes and datasets are available at: <https://github.com/Distance-awareNS/DNS/>.

### Benchmark Datasets:

In our experiments, we use four benchmark datasets- CiteSeer, Cora, PubMed and PPI. Among them, CiteSeer, Cora, and PubMed are citation-networks and PPI is a protein-protein interaction network. In the citation network, the nodes correspond to articles of different subjects, whereas the edges correspond to citations between those articles; consequently, the node prediction task on

this network is to predict the article subject. Meanwhile, the physical interaction between different proteins with their defined roles (cellular functions) on a specific human tissue <sup>1</sup> is represented using a protein-protein interaction network where the classification task is to predict the protein roles.

As discussed in Section 5, we focus our experiments on the largest connected component of these networks. Table 2 summarizes all the datasets with significant statistics where we see CiteSeer, Cora, and PubMed are sparse datasets with average degrees from 3.47 to 4.5, whereas PPI is quite dense with average degree 27.97.

### Synthetic Datasets:

We further analyze the performance of our DNS-based GRL model with varying graph density using three synthetic datasets, where we construct these synthetic datasets in two steps: Network Generation and Label Propagation.

**Network Generation:** We construct the synthetic networks by generating a node degree sequence that follows the power-law distribution. For our experiments, we use *networkx.utils.powerlaw\_sequence* to generate the degree sequence which takes two parameters: the number of nodes and the exponent of the power-law distribution, where we set the number of nodes as 2,000 and vary the exponent to generate varying networks with different density. After that, we use *networkx.expected\_degree\_graph* to construct a network from each degree sequence; whereas each network may have many disconnected components. To connect all the components of the network, we randomly choose one node from each disconnected component and connect them using minimum number of artificial edges.

**Label Propagation:** To evaluate the performance of our models on the downstream node classification task, we generate structure-induced node labels using a simple label propagation approach. Initially, we randomly select  $k$  seed nodes for  $k$  distinct classes. For sparse network, we choose  $k = 7$  classes, whereas, for moderate and dense networks, we choose  $k = 5$  and  $k = 4$  classes respectively. At each iteration, we propagate the node label to its adjacent unlabeled nodes. Consequently, we iterate this procedure until all the nodes get labeled. Therefore, the node labels are generated only using the structure information, such as the proximity from the seed node.

### Ablation Study:

We perform an ablation study of our DNS sampler by splitting the negative sampling probability into two parts; the splitting point is the pairwise distance for which DNS probability  $\approx$  UNS probability. In the first ablation model, we set negative sampling probability linearly proportional to the pairwise distance for nearby nodes while maintaining uniform negative sampling probability for the rest of the nodes. In the second ablation model, we set a uniform negative sampling probability for nearby nodes while setting DNS-like probability for distant nodes. Let us denote the first sampler as DNS-min since its negative sampling probability  $P_{min}(k|i) = \min(P_{DNS}(k|i), \frac{1}{n})$  and the second sampler as DNS-max that has negative sampling probability  $P_{max}(k|i) = \max(P_{DNS}(k|i), \frac{1}{n})$ . Both DNS-min and DNS-max samplers have higher separation than UNS sampler.

Figure 5 shows the node classification performance of different samplers with the DeepWalk model. The top row of Figure 5 shows the F1-Macro score of DeepWalk-UNS and DeepWalk-DNS with varying context size. As discussed in Section 4, we see the performance of the DeepWalk-DNS model decreases with increasing context window size. Moreover, low negative sampling probability for nearby nodes is not effective for the synthetic dense graph.

In the second row of Figure 5, we see the comparison of DNS, DNS-min, and DNS-max in terms of node classification performance. The DeepWalk-DNS-max follows the trend of the DeepWalk-UNS model performance for lower context windows, whereas, the DeepWalk-DNS-min model more likely follows the trend of the DeepWalk-DNS model in all the synthetic graphs.

---

<sup>1</sup>Instead of working on multiple graphs, we randomly select one PPI network corresponding to a specific human tissue.

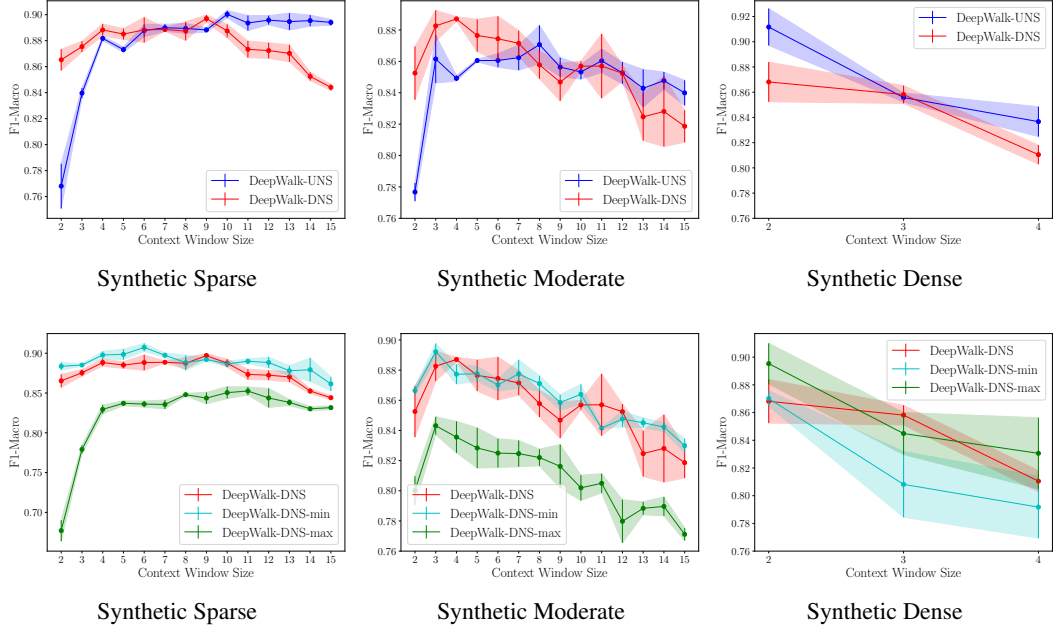


Figure 5: F1-Macro score plot with varying context window on Synthetic Sparse, Synthetic Moderate, and Synthetic Dense dataset. Competing models are DeepWalk-UNS, DeepWalk-DNS, and its variants DeepWalk-DNS-min, DeepWalk-DNS-max.

### $\gamma$ -linear Negative Sampling:

We perform an empirical study to visualize the effect of varying  $\gamma$  in  $\gamma$ -linear negative sampler on the synthetic datasets. We train the DeepWalk model with  $\gamma$ -linear negative sampler and denote it by  $\gamma$ -DNS. Moreover, we choose different values for  $\gamma$  from 0 to 1.25 for this experiment (the models are denoted by  $\gamma$ (value)-DNS). In this experiment, we denote the DeepWalk-DNS model by  $\gamma(1.0)$ -DNS. From Figure 6, we see that  $\gamma$  value closer to 1 follows the trend of the DeepWalk-DNS performance, whereas,  $\gamma$  value closer to 0 follows the trend of the DeepWalk-UNS model performance. Theoretically, the performance of the  $\gamma(0)$ -DNS based model should be close to the UNS based model, but there is deviation across runs that require further investigation.

### Hardware Specifications:

We ran our experiments in a single machine with 2 NVIDIA Titan RTX GPUs (24Gb of RAM) and 1 Intel(R) Xeon(R) W-2135 CPU (@ 3.70GHz). We use PyTorch with cuda-10.1 for our experiments. Overall, for small networks (CiteSeer, Cora, PPI and Synthetic networks), each training epochs on average takes one minute, whereas, for medium-size networks (PubMed), each training epochs take around 15 minutes. For our experiments, we report each accuracy with its mean and variance over 5 independent runs.

## References

Zhilin Yang, William W. Cohen, and Ruslan Salakhutdinov. Revisiting semi-supervised learning with graph embeddings. *CoRR*, abs/1603.08861, 2016. URL <http://arxiv.org/abs/1603.08861>.

Thomas N. Kipf and Max Welling. Semi-supervised classification with graph convolutional networks. *CoRR*, abs/1609.02907, 2016a. URL <http://arxiv.org/abs/1609.02907>.

Justin Gilmer, Samuel S. Schoenholz, Patrick F. Riley, Oriol Vinyals, and George E. Dahl. Neural message passing for quantum chemistry. *CoRR*, abs/1704.01212, 2017. URL <http://arxiv.org/abs/1704.01212>.

Alberto García-Durán and Mathias Niepert. Learning graph representations with embedding propagation. *CoRR*, abs/1710.03059, 2017. URL <http://arxiv.org/abs/1710.03059>.

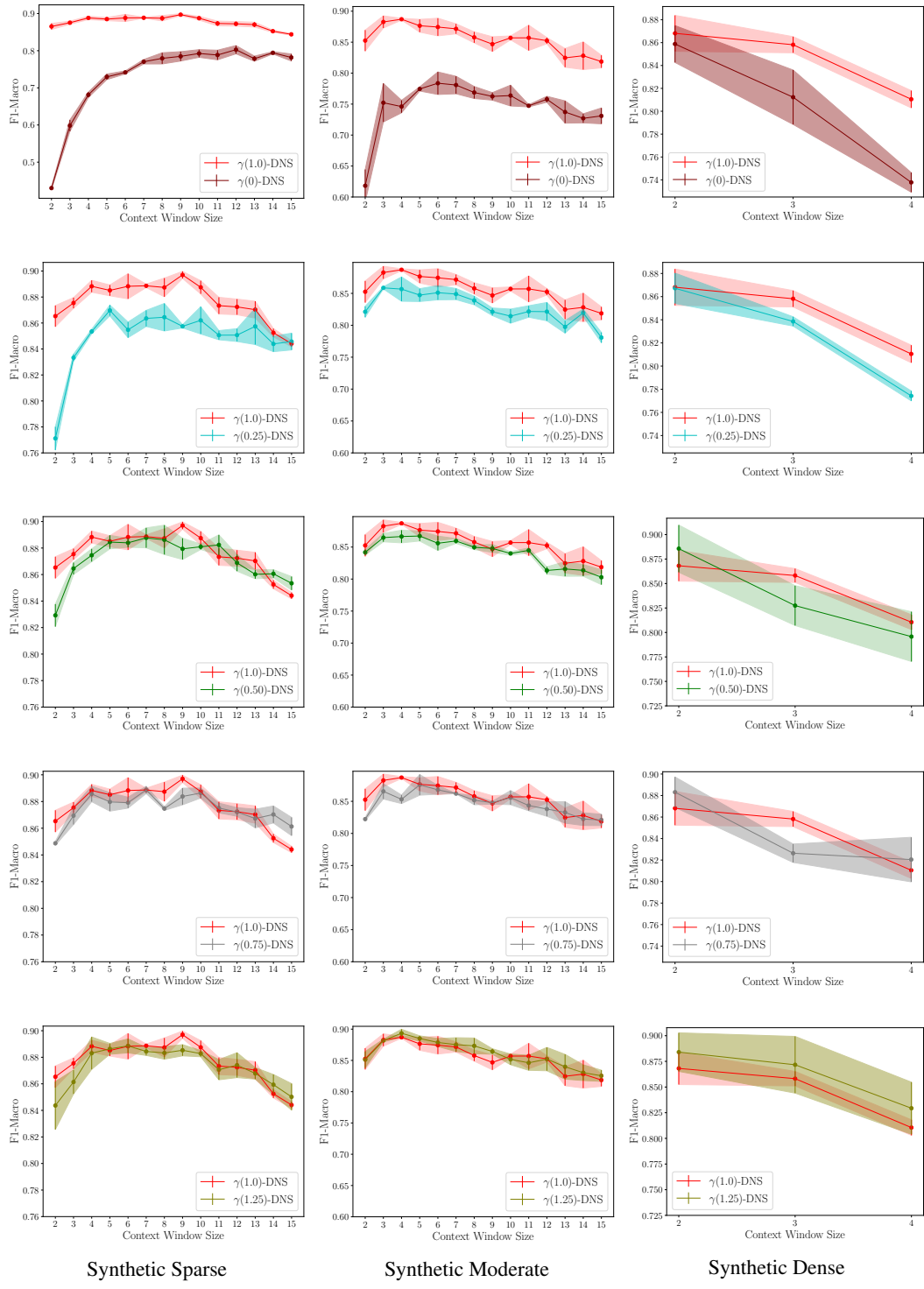


Figure 6: Node classification performance (F1-Macro score) comparison for various  $\gamma$ -linear sampler based models with varying context window on Synthetic Sparse, Synthetic Moderate, and Synthetic Dense dataset.

Will Hamilton, Zhitao Ying, and Jure Leskovec. Inductive representation learning on large graphs. In *Advances in neural information processing systems*, pages 1024–1034, 2017.

Petar Veličković, Guillem Cucurull, Arantxa Casanova, Adriana Romero, Pietro Lio, and Yoshua Bengio. Graph attention networks. *arXiv preprint arXiv:1710.10903*, 2017.

Tomas Mikolov, Kai Chen, Greg Corrado, and Jeffrey Dean. Efficient estimation of word representations in vector space. *arXiv preprint arXiv:1301.3781*, 2013.

Amr Ahmed, Nino Shervashidze, Shravan Narayananamurthy, Vanja Josifovski, and Alexander J Smola. Distributed large-scale natural graph factorization. In *Proceedings of the 22nd international conference on World Wide Web*, pages 37–48, 2013.

Shaosheng Cao, Wei Lu, and Qiongkai Xu. Grarep: Learning graph representations with global structural information. In *Proceedings of the 24th ACM international conference on information and knowledge management*, pages 891–900, 2015.

Mingdong Ou, Peng Cui, Jian Pei, Ziwei Zhang, and Wenwu Zhu. Asymmetric transitivity preserving graph embedding. In *Proceedings of the 22nd ACM SIGKDD international conference on Knowledge discovery and data mining*, pages 1105–1114, 2016.

Bryan Perozzi, Rami Al-Rfou, and Steven Skiena. Deepwalk: Online learning of social representations. In *Proceedings of the 20th ACM SIGKDD international conference on Knowledge discovery and data mining*, pages 701–710, 2014.

Sami Abu-El-Haija, Bryan Perozzi, Rami Al-Rfou, and Alex Alemi. Watch your step: Learning graph embeddings through attention. *CoRR*, abs/1710.09599, 2017. URL <http://arxiv.org/abs/1710.09599>.

Mohammadreza Armandpour, Patrick Ding, Jianhua Huang, and Xia Hu. Robust negative sampling for network embedding. In *Proceedings of the AAAI Conference on Artificial Intelligence*, volume 33, pages 3191–3198, 2019.

Thomas N Kipf and Max Welling. Variational graph auto-encoders. *arXiv preprint arXiv:1611.07308*, 2016b.

Petar Veličković, William Fedus, William L Hamilton, Pietro Liò, Yoshua Bengio, and R Devon Hjelm. Deep graph infomax. *arXiv preprint arXiv:1809.10341*, 2018.

Aditya Grover and Jure Leskovec. node2vec: Scalable feature learning for networks. In *Proceedings of the 22nd ACM SIGKDD international conference on Knowledge discovery and data mining*, pages 855–864, 2016.

Jian Tang, Meng Qu, Mingzhe Wang, Ming Zhang, Jun Yan, and Qiaozhu Mei. Line: Large-scale information network embedding. In *Proceedings of the 24th international conference on world wide web*, pages 1067–1077, 2015.

Zellig S Harris. Distributional structure. *Word*, 10(2-3):146–162, 1954.

Michael Gutmann and Aapo Hyvärinen. Noise-contrastive estimation: A new estimation principle for unnormalized statistical models. In *Proceedings of the Thirteenth International Conference on Artificial Intelligence and Statistics*, pages 297–304, 2010.

Edsger W Dijkstra. A note on two problems in connexion with graphs. *Numerische mathematik*, 1(1):269–271, 1959.

M. L. Fredman and R. E. Tarjan. Fibonacci heaps and their uses in improved network optimization algorithms. In *25th Annual Symposium on Foundations of Computer Science, 1984.*, pages 338–346, 1984.

Marinka Zitnik and Jure Leskovec. Predicting multicellular function through multi-layer tissue networks. *CoRR*, abs/1707.04638, 2017. URL <http://arxiv.org/abs/1707.04638>.

Matthias Fey and Jan E. Lenssen. Fast graph representation learning with PyTorch Geometric. In *ICLR Workshop on Representation Learning on Graphs and Manifolds*, 2019.

Shuang-Hong Yang, Bo Long, Alex Smola, Narayanan Sadagopan, Zhaohui Zheng, and Hongyuan Zha. Like like alike: joint friendship and interest propagation in social networks. In *Proceedings of the 20th international conference on World wide web*, pages 537–546, 2011.

Ioannis Konstas, Vassilios Stathopoulos, and Joemon M Jose. On social networks and collaborative recommendation. In *Proceedings of the 32nd international ACM SIGIR conference on Research and development in information retrieval*, pages 195–202, 2009.

Lars Backstrom and Jure Leskovec. Supervised random walks: predicting and recommending links in social networks. In *Proceedings of the fourth ACM international conference on Web search and data mining*, pages 635–644, 2011.

David Liben-Nowell and Jon Kleinberg. The link-prediction problem for social networks. *Journal of the American society for information science and technology*, 58(7):1019–1031, 2007.

Chris Stark, Bobby-Joe Breitkreutz, Teresa Reguly, Lorrie Boucher, Ashton Breitkreutz, and Mike Tyers. Biogrid: a general repository for interaction datasets. *Nucleic acids research*, 34(suppl\_1):D535–D539, 2006.

Predrag Radivojac, Wyatt T Clark, Tal Ronnen Oron, Alexandra M Schnoes, Tobias Wittkop, Artem Sokolov, Kiley Graim, Christopher Funk, Karin Verspoor, Asa Ben-Hur, et al. A large-scale evaluation of computational protein function prediction. *Nature methods*, 10(3):221–227, 2013.